BMC Chemistry

RESEARCH Open Access

Adsorption of heavy metals from wastewater using reduced graphene oxide@titanate hybrids in batch and fixed bed systems

Xiutao Yang[1], Pan Liu[1,2] and Hongwen Yu[1*]

Abstract

Wastewater contaminated by heavy metal ions poses serious threats to the ecosystem, needing to be well disposed of. In this study, reduced graphene oxide@titanate hybrids (rGOTHs) are synthesized to efficiently remove heavy metals from wastewater in batch and fixed bed systems. The size of prepared rGOTHs is large as hundreds of microns, which is beneficial for separation and application in batch and fixed bed system. In the batch studies, rGOTHs exhibits the fast adsorption rate and high adsorption capacity towards heavy metals, in which the adsorption kinetic and isothermal are best fitted to Pseudo-second-order kinetic model and Langmuir model, respectively. The maximum adsorption capacities of rGOTHs for Pb(II), Cd(II) and Cu(II) are 530.5, 201 and 130.5 mg/g at 298 K and pH 5, respectively. In addition, the exhausted adsorbent can be easily regenerated in alkaline hydrothermal process and the high removal efficiency is almost reserved after six cycles. Moreover, rGOTHs presents higher selective adsorption towards Pb(II) than other ions. Adsorption mechanisms are revealed to be ions exchange, electrostatic interaction, and coordination. In the fixed bed experiments, the effective treatment volume of rGOTHs-loaded column reaches to 2760 BV (15.45 L) for single Pb(II) polluted battery manufactory wastewater and 2280 BV (12.76 L) for multiple heavy metal polluted estuary effluent, before Pb(II) concentration exceeds the discharge limit of 1 mg/L. Our study demonstrates the great potential of rGOTHs to be applied in practical treatment of wastewater contaminated by heavy metal ions.

Keywords Titanate, Graphene oxide, Heavy metals, Adsorption

Introduction

Nowadays, facing the worse environment condition caused by discharge of wastewater containing multiple pollutants, especially toxic heavy metals, environmental pollution and control has gradually become a big challenge for human [1]. The inherent non-degradable nature of heavy metals makes them be persistent and gradually accumulate along the ecological chain, resulting in serious threats to all species in nature, especially to human [2, 3]. Heavy metals pollution mainly comes up with industrial waste generated by battery manufacturing, mining, electroplating and oil refining. Therefore, to control heavy metals pollution in a real sense, the wastewater contaminated by heavy metal ions must be disposed of before discharge, meeting the government standards for the allowance limit [4].

Many techniques, such as adsorption [5], coagulation-flocculation [6], electrochemical treatment [7] and chemical precipitation [8], were used to eliminate heavy metal ions from wastewater. Considering the efficiency

*Correspondence:
Hongwen Yu
yuhw@iga.ac.cn
[1]Northeast Institute of Geography and Agroecology, Chinese Academy of Sciences, 4888 Shengbei Rd, Changchun 130102, P. R. China
[2]University of Chinese Academy of Sciences, Beijing 100049, P. R. China

and cost, adsorption is one of the wildly accepted techniques in the laboratory and practical application [9, 10]. In recent years, many novel and high-efficient nanomaterials such as MOF, COF, mesoporous metal oxides and titanate have been developed to purify the wastewater contaminated by heavy metal ions [11–14]. However, those nanomaterials are portable in the environment and difficult to separate and reclaim, which gives rise to high hazard to the ecosystem [15, 16]. Moreover, nano-sized adsorbents suffer from severe pressure drop in column processes, which hinders their practical application. Hence, nanomaterials are generally loaded on large scale supports, such as zeolite, activated carbon and aluminum, to enhance the reclaim ability and applicability [17, 18]. Unfortunately, the hybrids are suffering a significant loss of adsorption efficiency towards target heavy metals due to the poor affinity of traditional porous supports and sever aggregation of impregnated nanoparticles [19]. Therefore, there is a need to devise ways of fabricating novel hybrids with large size and high adsorption capacity.

Graphene oxide (GO) is an attractive nanomaterial to fabricate hybrids for pollutants elimination due to their fascinating features, such as thin 2D plane structure, light weight, large specific surface area and abundant oxygenated function groups [20]. In recent years, GO-based hybrids are proved to be excellent adsorbents for the three main reason [21]: (I) The utilization of GO nanosheets as support templates to carry nanoparticles can reduce their serious aggregation, promoting the proper distribution of active functional sites [22, 23]; (II) GO nanosheets can be used as building block to form 3D composites with massive morphology, which is beneficial for reclaim from water and application in fix bed [24]; (III) GO nanosheets themselves show high affinity to many pollutants [25]. For example, SiO_2/graphene composite was prepared and exhibited maximum adsorption capacity as 113.6 mg/g towards Pb(II) [26]; Huang et al. feasibly prepared Magnetic graphene oxide/MgAl-LDH and the optimal removal capacity towards Pb(II), Cd(II) and Cu(II) reached 192.3, 45.05 and 23.04 mg/g respectively [27]; Lellala et al. fabricated Fe_3O_4-N-doped GO composites by sol-gel assisted microwave method and this novel adsorbent can remove Pb(II), Cd(II), Cu(II), Zn(II) and Ni(II) with adsorption capacities of 190, 67, 95, 100 and 85 mg/g respectively, under optimal condition [28]. However, the adsorption capacity of those GO-based hybrids is still lower than expected. The adsorption efficiency of GO-based hybrid towards heavy metal needs to be put forwards by designing novel composites.

Titanates nanomaterials are well known as nano-adsorbent with high performance in eliminating the heavy metals from wastewater due to their excellent ion-exchange capacity, large specific surface area and abundant -OH group [29–31]. However, few works focus on fabrication novel GO-titanate hybrids for high-efficiency adsorption of heavy metals from wastewater in batch and fixed bed systems [32]. Herein, novel reduced graphene oxide@titanate hybrids (rGOTHs) were fabricated through two step procedures and performed well in removing heavy metals from wastewater in both batch and fixed bed systems. The objectives of this research were: (I) to adequately characterize the microstructure of rGOTHs with advanced techniques; (II) to systematically investigate the adsorption behaviors of rGOTHs towards heavy metals; (III) to reveal the adsorption mechanism of rGOTHs towards heavy metals by spectroscopy analyses. This novelty of this study lies in development of the novel rGOTHs with high performance, which could feasible elimination of heavy metal from wastewater in both batch and fixed bed systems. With proper synthesis protocol, GO nanosheet and titanate nanosheets formed into novel 3D hybrid, not only retaining the high adsorption capacity towards heavy metal, but also enhancing the applicability through macro-sized morphology.

Materials and methods

Materials, reagents, and characterization

The details of materials and chemical reagents were presented in supplementary information. All chemical reagents were of analytical grade and with no further purification. The details of characterization, including scanning electron microscopy (SEM), transmission electron microscopy (TEM), X-ray diffraction (XRD), X-ray photoelectron spectroscopy (XPS), Fourier transform infrared spectroscopy (FTIR) and thermogravimetric analysis (TGA) were illustrated in supplementary information.

Synthesis of reduced graphene oxide@titanate hybrids (rGOTHs)

Firstly, the graphene oxide (GO) solution was prepared by a modified Hummer's method. The prepared GO were thoroughly washed with water and ethanol, then re-dispersed into solution of 400 mL ethanol and 5 mL H_2O (containing 250 mg GO and 0.3 g of Hydroxypropyl cellulose). Afterwards, 15 mL of tetrabutyl titanate (TBOT) were dissolved into 50 mL of ethanol, then added dropwise into the GO suspension. The temperature of suspension was heated to 80 °C and maintained for 100 min, during which TBOT was hydrolyzed to $Ti(OH)_x$ and coated on GO nanosheets. The precipitates were collected by centrifugal separation with 320 mL of ethanol and 320 mL of water three times, respectively. The collected precipitates were dispersed in 30 mL NaOH solution (1 M), then stirred for 30 min and transferred into 50-mL autoclave (containing 0.8 g dry mass of precipitates). Then, the autoclave was sealed and heated at 160

℃ for 6 h. After cooling to room temperature, the products were rinsed with 320 mL of water and 320 mL of ethanol three times, respectively. The final products were obtained by lyophilization of dispersing solution (100 mL), denoted as rGOTHs15. In comparison, 5 mL or 10 mL of TBOT were dissolved into 50 mL of ethanol, then added dropwise into the GO suspension. Afterwards the subsequent synthesis followed the procedure of rGOTHs15, the obtained products were denoted as rGOTHs5 and rGOTHs10, respectively.

Batch adsorption experiments

The batch adsorption experiments were conducted to investigate adsorption behaviors of Pb(II), Cd(II) and Cu(II) onto rGOTHs using a constant temperature incubator (130 rpm, 25 °C) with 50 mL conical flasks. The detailed batch adsorption experiment conditions were presented in supplementary information.

Fixed bed adsorption experiments

Fixed bed column packed with rGOTHs (2 g placed in one column) was utilized to dynamiclly process artificial battery wastewater containing Pb(II) (30.548 mg/L), Na^+ (16.67 mg/L), K^+ (6.511 mg/L), Ca^{2+} (68.2 mg/L), Mg^{2+} (12.265 mg/L) and estuary effluent from industries areas containing Pb(II) (29.33 mg/L), Cd(II) (7.42 mg/L), Cu(II) (21.3 mg/L), Zn(II) (25.6 mg/L), Na^+ (296.2 mg/L), Ca^{2+} (64.21 mg/L), Mg^{2+} (39.13 mg/L), separately. The pH of two synthetic wastewater was adjusted to 5.0 prior to application. The residual concentrations of heavy metals were measured by ICP-OES (ICP-5000, Focused Photonics, Inc., China).

Results and discussions

Characterization of rGOTHs composites

The prepared GO nanosheets possessed ultrathin and wrinkled 2D structure (Fig. S1) and were applied as supported template for synthesizing rGO@titanate hybrids (rGOTHs). The SEM images (Fig. 1a-c) showed that all rGOTHs are three-dimensional sheet-stacked composites with large size of hundreds of microns. According to the XRD patterns (Fig. 1d), characteristic peaks of all rGOTHs clearly occurred at $2\theta = 9.2°$, 24.6°, 26.7° and 47.5°, which can be assigned to (001), (201), (003), (020) respectively of sodium trititanate ($Na_xH_{2-x}Ti_3O_7{\cdot}H_2O$) [33, 34]. In comparison, the characteristic peak at 11.37° for (002) graphene oxide was decreased, indicating the reduction of graphene oxide [35]. As shown in Fig. S2, comparing with GO, the FTIR spectrum of rGOTHs appended two new adsorption bands at 887 and 454 cm^{-1}, corresponding to Ti-O stretching vibration and [TiO_6] octahedron vibration of titanate materials [17], while disappeared adsorption bands at 1732 cm^{-1}, and inherited attenuate adsorption bands between 1638 and 1000 cm^{-1}. Those changes indicated the combination of GO and titanate, and the existence of oxygenic functional group on the surface of GOTNs [36]. From TGA curves (Fig. 1e), as GO can be thoroughly removed in

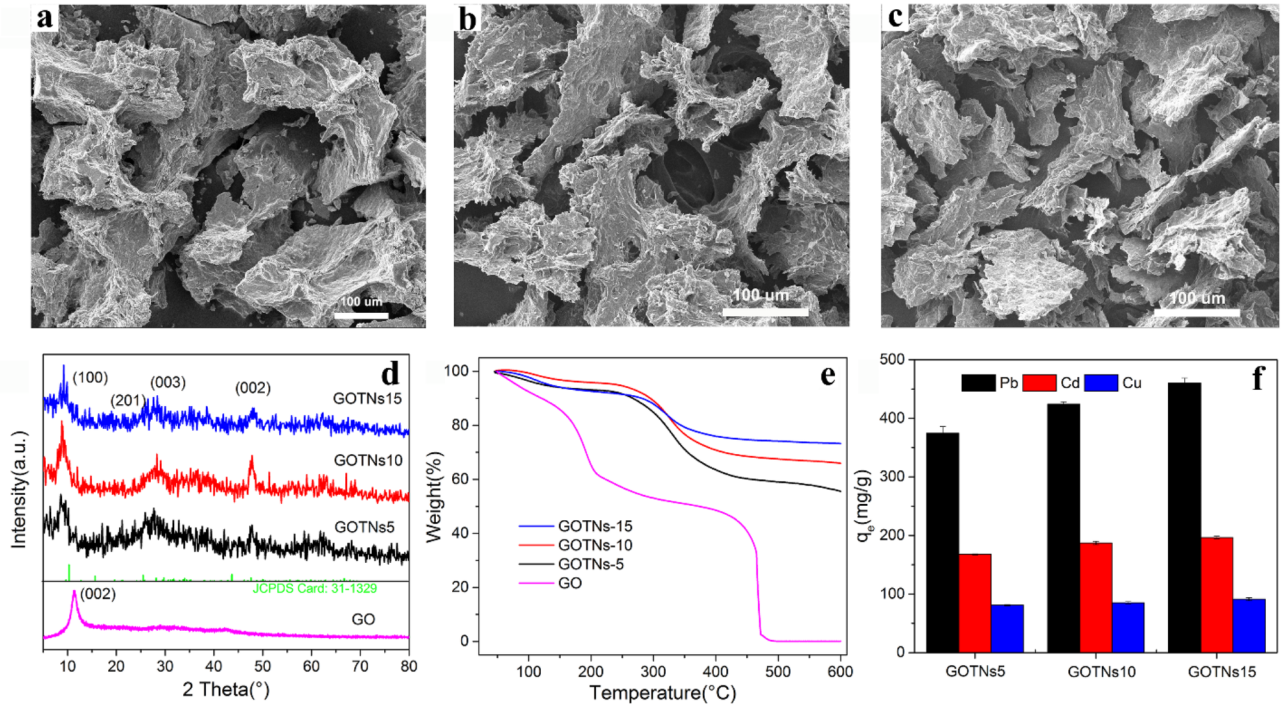

Fig. 1 SEM image of (**a**) rGOTHs15, (**b**) rGOTHs10 and (**c**) rGOTHs5; (**d**) XRD patterns, (**e**) TGA curves and (**f**) Pb(II), Cd(II), Cu(II) adsorption capacities of all rGOTHs

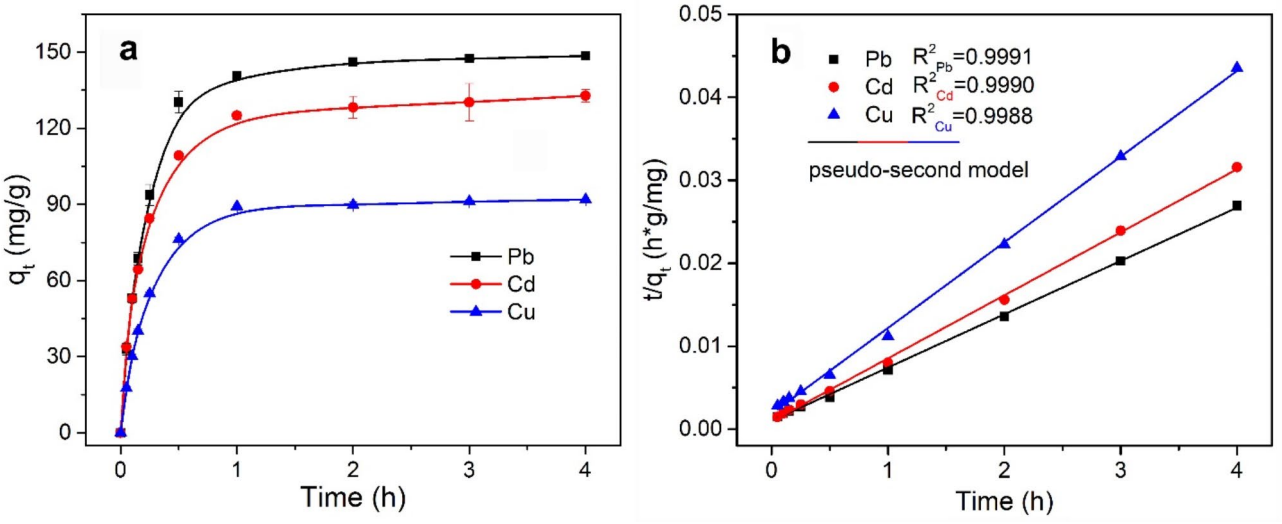

Fig. 2 (**a**) Adsorption kinetics for adsorption of Pb(II), Cd(II) and Cu(II) on rGOTHs15 in batch experiments and (**b**) the linear pseudo-second model fitting

Table 1 Kinetic parameters for the adsorption of Pb(II), Cd(II) and Cu(II) by rGOTHs15 at 298 K

Kinetic models	Parameters	Pb(II)	Cd(II)	Cu(II)
Pseudo-first-order kinetic model	k_1 (h^{-1})	1.186	1.072	1.080
	$q_{e,cal}$[a] (mg/g)	67.1	63.5	42.5
	R^2	0.8856	0.9094	0.8521
Pseudo-second-order kinetic model	k_2 (g/(mg·h))	0.0412	0.0622	0.0571
	$q_{e,cal}$ (mg/g)	155.7	131.6	96.8
	R^2	0.9991	0.9990	0.9988
	$q_{e,exp}$[b](mg/g)	148.4	132.8	91.9

[a] Model simulated equilibrium capacity of Pb(II), Cd(II) and Cu(II)

[b] Experimental equilibrium uptake of Pb(II), Cd(II) and Cu(II)

the thermal process above 500 °C, the content of titanate in rGOTNs5, rGOTNs10 and rGOTNs15 were determined to be 55.5%, 65.9% and 73.3%, respectively. With the increase of titanate content, rGOTHs showed better adsorption capacity. As shown in Fig. 1f, the adsorption capacity of rGOTHs15 is 460.1 mg/g, 196.5 mg/g and 91.2 mg/g for Pb(II), Cd(II) and Cu(II) respectively, which are better than rGOTHs5 (increased 22.9%, 16.7% and 12.3%) and rGOTHs10 (increased 8%, 4.8% and 1%). Considering the adsorption capacity of each rGOTHs composite, rGOTHs15 is chosen to be the best adsorbent for adsorption of heavy metal ions.

The elemental mapping images and EDX from SEM (Fig. S3) suggested the existence and homogenous distribution of C, O, Na and Ti elements in rGOTHs15. The fitting analysis based on BET revealed the specific surface area, total pore volume and pore diameter of rGOTHs15 are 10.6 m^2 g^{-1}, 0.013 cm^3 g^{-2} and 3.6 nm, respectively (Fig. S4). The combination between rGO and titanate is further proved by TEM (Fig. S5), where titanate nanosheets (distinctive lattice distance of 0.79 nm) with few layers (4–10) are supported on rGO. Furthermore, rGOTHs15 can easily be quickly separated from aqueous solution by sedimentation, owing to intrinsic large particle size (Fig. S6). Considering the high adsorption capacity and easy separation, the potential of rGOTHs15 in treatment of heavy metal contaminated wastewater was promising.

Adsorption kinetics and isotherms

The adsorption kinetics experiments of Pb(II), Cd(II) and Cu(II) on rGOTHs15 were carried out and investigated by pseudo-first order model and pseudo-second order model. The results are shown in Fig. 2; Table 1. The adsorption behaviors of Pb(II), Cd(II) and Cu(II) on rGOTHs15 shows similar tendency as their adsorption rate is rapid in the first 30 min and slowing down beyond 30 min (Fig. 2a). The pseudo-second order model (Fig. 2b) shows better correlation coefficients than the pseudo-first order model (Fig. S7), indicating chemisorption and surface complexation might be the rate limiting step for Pb(II), Cd(II) and Cu(II) adsorption on rGOTHs15.

Figure 3 presents the adsorption isotherms of Pb(II), Cd(II) and Cu(II) on rGOTHs15. With the initial heavy metal concentrations increasing, the adsorption capacity of rGOTHs15 towards Pb(II), Cd(II) and Cu(II) is increased until saturated. The L-type isotherms with saturated adsorption capacity implies the adsorption sites on rGOTHs15 are limited and the adsorption behavior aligns well with the Langmuir model, which describes adsorption as a monolayer coverage on a homogeneous surface. Moreover, according to the detail parameters given in Table 2, the Langmuir model fits better with the adsorption isotherm data for Pb(II), Cd(II) and Cu(II) on rGOTHs15 than Freundlich model, suggesting that the adsorption process was predominant monolayer. Herein, the monolayer adsorption model is favored for

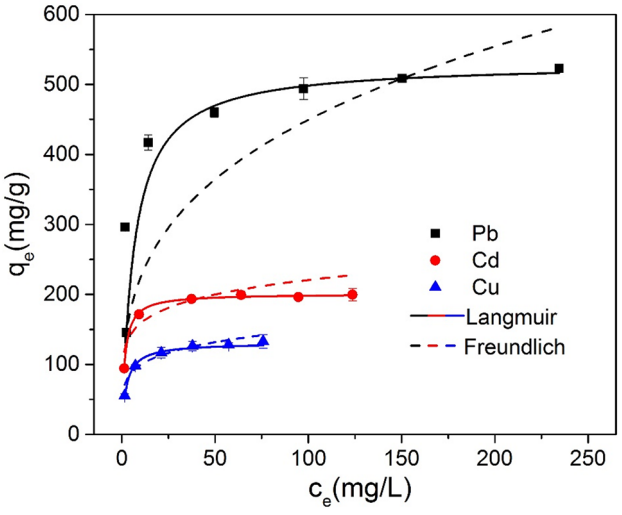

Fig. 3 Adsorption equilibrium isotherm for adsorption of Pb(II), Cd(II) and Cu(II) on rGOTHs15, and the fitting by Langmuir and Freundlich model

Table 2 Isothermal parameters for the adsorption of Pb(II), Cd(II) and Cu(II) by rGOTHs15 at 298 K

Isotherm models	Parameters	Pb(II)	Cd(II)	Cu(II)
Langmuir	q_{max} (mg/g)	530.5	201.0	130.9
	K_L(L/mg)	0.155	0.690	0.437
	R^2	0.997	0.998	0.989
Freundlich	K_F ((mg/g)·(L/mg)$^{1/n}$)	111.6	114.3	66.0
	n	3.305	6.998	5.662
	R^2	0.996	0.799	0.826

rGOTHs15, which is coincidence with many rGO-based and titanate-based adsorbents [37–39]. The calculated maximum adsorption capacity of rGOTHs15 at 298 K are 530.5, 201, 130.5 mg/g (2.56, 1.79, 2.03 mmol/g) for Pb(II), Cd(II) and Cu(II), respectively. The larger adsorption capacity of rGOTHs15 for Pb(II) than Cd(II) and Cu(II) in the same conditions indicated the higher affinity for Pb(II).

The adsorption capacities of as-prepared rGOTHs15 for Pb(II), Cd(II) and Cu(II) are similar to that of titanate nanomaterials (Table S1). When compared with various graphene oxide-based adsorbents cited in Table 3, the as-prepared rGOTHs15 is more effective, which demonstrates its potential in eliminating heavy metals from wastewater. The high loading mass of titanate and outstanding cation-exchanging ability guarantee the superior performance of rGOTHs than the specific alternatives like GO-zirconium phosphate or Fe_3S_4/rGO.

Effects of pH and coexisting ions

Generally, the environmental conditions, such as pH, greatly affect the adsorption performance of adsorbents to remove heavy metals. In a solution with different pH, both the species of heavy metals and the properties of adsorbents (especially surface charge) can be affected. The pH of heavy metals solution was controlled from 2 to 6 to conduct the adsorption experiments of rGOTHs15. As shown in Fig. 4a, the removal ratio of three heavy metals increase with an increasing pH and reached maximum at pH 5 (98.7%, 87.0% and 64.96% for Pb(II), Cd(II) and Cu(II), respectively). When pH at 6, the adsorption capacities of rGOTHs toward Pb(II), Cd(II) and Cu(II) are similar to that of pH at 5. When the solution pH is 2, rGOTHs15 shows extremely low sorption ratio for Cd(II) and Cu(II), while attaining only 40.4% for Pb(II). The increasing H^+ could compete the active sites on rGOTHs with Pb(II), Cd(II) and Cu(II). However, rGOTHs still have a higher capability to remove Pb(II) in relatively strong acid condition. The results also indicate that extremely strong acid treatment could be applied to elute rGOTHs15 after adsorption.

Common cations and natural organic matters such as Na^+, K^+, Ca^{2+}, Mg^{2+}, Cl^-, SO_4^{2-} and humic acid (HA) always exist in the aquatic systems, so investigating the influence of coexisting ions and HA on adsorption ability of rGOTHs15 towards Pb(II), Cd(II) and Cu(II) was

Table 3 The adsorption capacities of Pb(II), Cd(II) and Cu(II) on recently reported graphene oxide-based adsorbents

Sorbents	Conditions		Maximum sorption capacities (mg/g)			References
	pH	Temperature	Pb	Cd	Cu	
Fe_3O_4/SiO_2-GO	6	45 °C	385.1	128.2		[22]
SiO_2/graphene	6	25 °C	113.6			[26]
3D GO/TiO_2	5.2	25 °C	199.2			[40]
SH-graphene bio-sponge[a]	5.3	21 °C	101	103		[41]
SA-PAM/GO hydrogel	5.3	21 °C	240.7		68.7	[42]
GO/MgAl-LDH/Fe_3O_4	5–6	25 °C	192.3	23	45.1	[27]
Fe_3O_4/NGO[b]	6	25 °C	190	67	95	[28]
rGO-PDTC/Fe_3O_4[c]	6	25 °C	147.1	116.3	113.6	[43]
Fe_3S_4/rGO	6	25 °C	285.7			[44]
GO-zirconium phosphate	6	25 °C	363.4	232.2	328.56	[45]
rGO@Titanate hybrids	5	25 °C	530.5	201.0	130.5	This study

[a] Containing Alginate/rGO/Fe_3O_4 composite; [b] NGO: N-doped graphene oxide; [c] PDTC: polydithiocarbamate

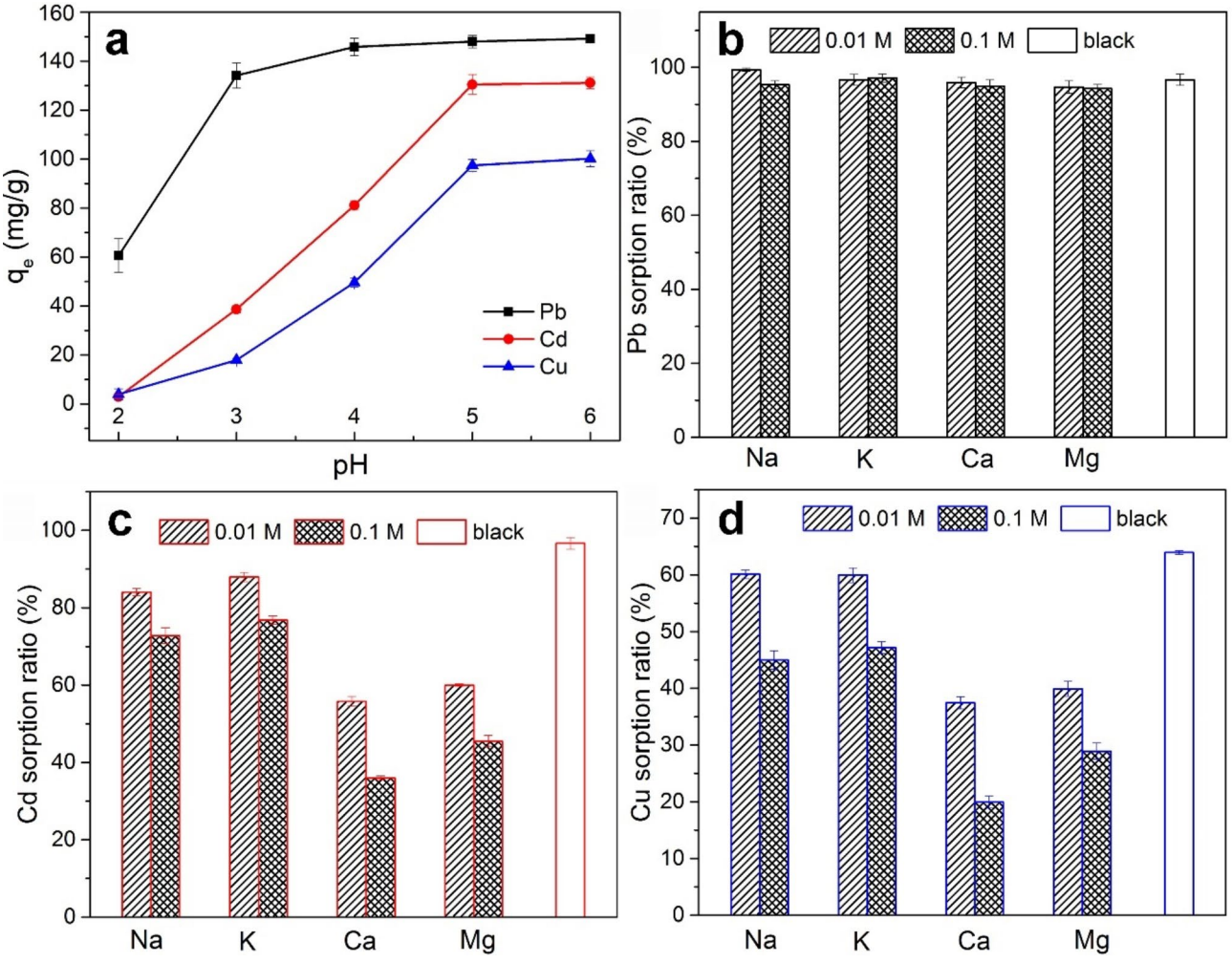

Fig. 4 Effect of pH (**a**) and coexisting ions on adsorption ability of rGOTHs15 towards (**b**) Pb(II), (**c**) Cd(II) and (**d**) Cu(II)

performed. Figure 4b-d demonstrates that coexisting Na^+, K^+, Ca^{2+}, Mg^{2+} have limited impact on adsorption ability of rGOTHs15 towards Pb(II). Compared to monovalent Na^+, K^+, the divalent Ca^{2+}, Mg^{2+} influences significantly on the removal capacity of rGOTHs15 towards Cd(II) and Cu(II), due to the stronger competition of divalent ions on active adsorption sites. Moreover, increasing concentration of coexisting ions would also decrease the adsorption capacity of rGOTHs15 towards Cd(II) and Cu(II). Fig. S8a-b exhibites the effect of Cl^-, SO_4^{2-} and HA on adsorption process. Cl^- and SO_4^{2-} have little effect on adsorption capacity of rGOTHs15 towards Cd(II) and Cu(II). HA promotes the adsorption capacity of rGOTHs15 towards Pb(II), Cd(II) and Cu(II), while the positive effect is more obvious when the concentration is 1 mg C/L than 10 mg C/L. It can be assumed that the formation of HA-Metal complex on the surface of rGOTHs promote the adsorption in the lower concentration of HA, but high concentration of HA may result in the instability of HA–Metal colloid molecular [46].

Recycling performance

The recycling ability is critical to evaluate the applicability of adsorbents. In this study, 0.1 M HCl was applied to elute rGOTHs15 loaded with Pb(II), Cd(II) and Cu(II). Since Na^+ in rGOTHs15 is consumed by ions exchange during the adsorption process, regeneration was conducted in 1 M NaOH hydrothermal treatment. As shown in Fig. 5, the sorption ratio of Pb(II), Cd(II) and Cu(II) are 94.0%, 80.7% and 65.5%, respectively, after six cycles. The excellent recycling ability proved that rGOTHs15 can be applied in sewage treatment.

Effect of initial concentration and dosage on competitive adsorption

The mixed heavy metals solution (Pb(II), Cd(II), Cu(II), Zn(II) and Ni(II)) with same initial concentration (30–200 mg/L) was prepared to evaluate the performance of rGOTHs15 in competitive adsorption. As shown in Fig. 6a, with increasing ions concentration, rGOTHs15 possesses enhanced adsorption capacity towards Pb(II),

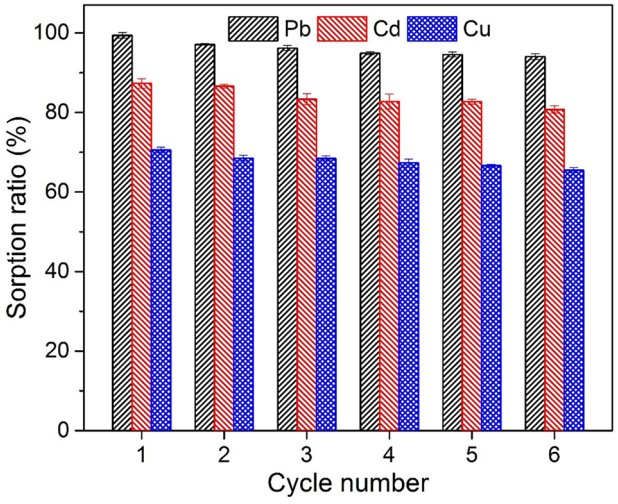

Fig. 5 Recycling performance of adsorption of Pb(II), Cd(II) and Cu(II) by rGOTHs15

while a declines was observed towards the other four heavy metal ions. As shown in Table 4, comparing the distribution ratio of specific heavy metal ions ($D_{M(II)}$), the affinity of the heavy metals on rGOTHs15 was in the following order Pb(II) > > Cd(II) ≈ Cu(II) > Zn(II) > > Ni(II). The affinity order may be ascribed to the differences in ionic radius and hydration energy. Metal ions with lower hydration energy have smaller hydrated ionic radius and are more likely to depolarize both from the hydration shell of metal ions and the sorbent surface [47, 48]. Furthermore, the selectivity coefficients $\beta_{Pb(II)/M(II)}$ at all initial concentrations are markedly greater than 1 and exhibit a rapid escalation with an increase in initial concentration, indicating a pronounced preference of rGOTHs15 for Pb(II) in solutions containing multiple metals [49].

A certain mass of rGOTHs15 cannot remove all heavy metals to reach the strict standard of discharge limit, so

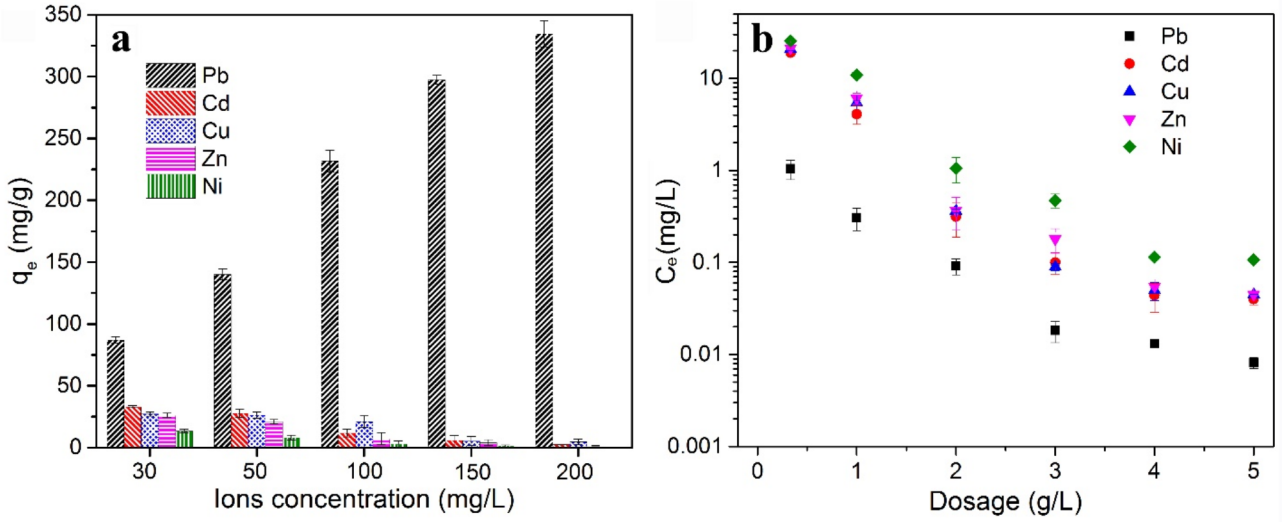

Fig. 6 (**a**) Effect of initial concentration and (**b**) dosage on competitive adsorption of Pb(II), Cd(II), Cu(II), Zn(II) and Ni(II) by rGOTHs15

Table 4 Competitive adsorption of Pb(II), Cd(II), Cu(II), Zn(II), and Ni(II) on rGOTHs15 with different initial concentration and adsorbent concentration

Dos-age (g/L)	Heavy metal ions	30 mg/L		50 mg/L		100 mg/L		150 mg/L		200 mg/L	
		D	*β*	*D*	*β*	*D*	*β*	*D*	*β*	*D*	*β*
0.333	Pb(II)	83.09	-	42.68	-	10.18	-	5.855	-	8.692	-
	Cd(II)	1.743	47.67	0.679	62.88	0.122	82.74	0.04	145.9	0.017	507.1
	Cu(II)	1.306	63.63	0.638	66.91	0.225	45.26	0.036	162.8	0.032	273.9
	Zn(II)	1.232	67.46	0.487	87.66	0.074	137.5	0.027	217.3	0.010	806.6
	Ni(II)	0.525	158.3	0.172	247.7	0.029	345.4	0.008	698.8	0.0015	5576
C_0 (mg/L)		1 g/L		2 g/L		3 g/L		4 g/L		5 g/L	
		D	*β*	*D*	*β*	*D*	*β*	*D*	*β*	*D*	*β*
30	Pb(II)	109.4	-	78.75	-	217.4	-	247.4	-	269.5	-
	Cd(II)	6.319	17.31	47.11	1.672	99.99	2.175	171.8	1.439	149.7	1.800
	Cu(II)	4.472	24.45	40.81	1.930	100.6	2.162	148.5	1.665	133.8	2.015
	Zn(II)	3.918	27.91	40.29	1.954	54.84	3.965	166.7	1.483	109.4	2.462
	Ni(II)	1.747	62.61	13.73	5.735	20.98	10.36	65.63	3.768	55.92	4.818

different dosages of rGOTHs15 were applied to dispose of Pb(II), Cd(II), Cu(II), Zn(II) and Ni(II) mixed solution with initial concentration of 30 mg/L. The residual heavy metals were measured and shown in Fig. 6b. When 3 g/L dosage was applied, the residual concentrations of the five heavy metals can meet the minimum standard set by the World Health Organization (WHO) and Environmental Protection Agency (EPA) [50]. With increasing dosage in a multi-metal solution, the distribution ratio $D_{M(II)}$ of five heavy metal ions were increasing (Table 4), indicating the potential of rGOTHs15 in simultaneously removing multiple heavy metal ions. In the multi-metal system, rGOTHs15 adsorbed Pb(II) as the first priority followed by the other heavy metals.

Adsorption mechanism

FTIR and XPS were conducted to explain the interaction mechanism between rGOTHs15 and heavy metals. From Fig. 7a, FTIR spectrum of rGOTHs15 shows a clear peak at 887 cm^{-1}, which represents the four-coordinated Ti-O stretching vibration with Na^+ coordinated to the non-bridging oxygen atom structure ($-TiO(ONa)_2$) [51]. The disappearance of this peak after Pb(II), Cd(II) and Cu(II) indicates that the interlayer structure of rGOTHs15 is changed, implying that ions exchange between Na^+ in rGOTHs15 and heavy metal ions has occurred in aqueous solution. Further characterization by XPS confirms the ion exchange process (Fig. 7b), where the Na 1s peak of rGOTHs disappears and corresponding Pb 4f, Cd 3d and Cu 2p peaks appear after adsorption of Pb(II), Cd(II) and Cu(II). Apart from ion exchange, the oxygen-containing groups of rGOTHs15 play an important role

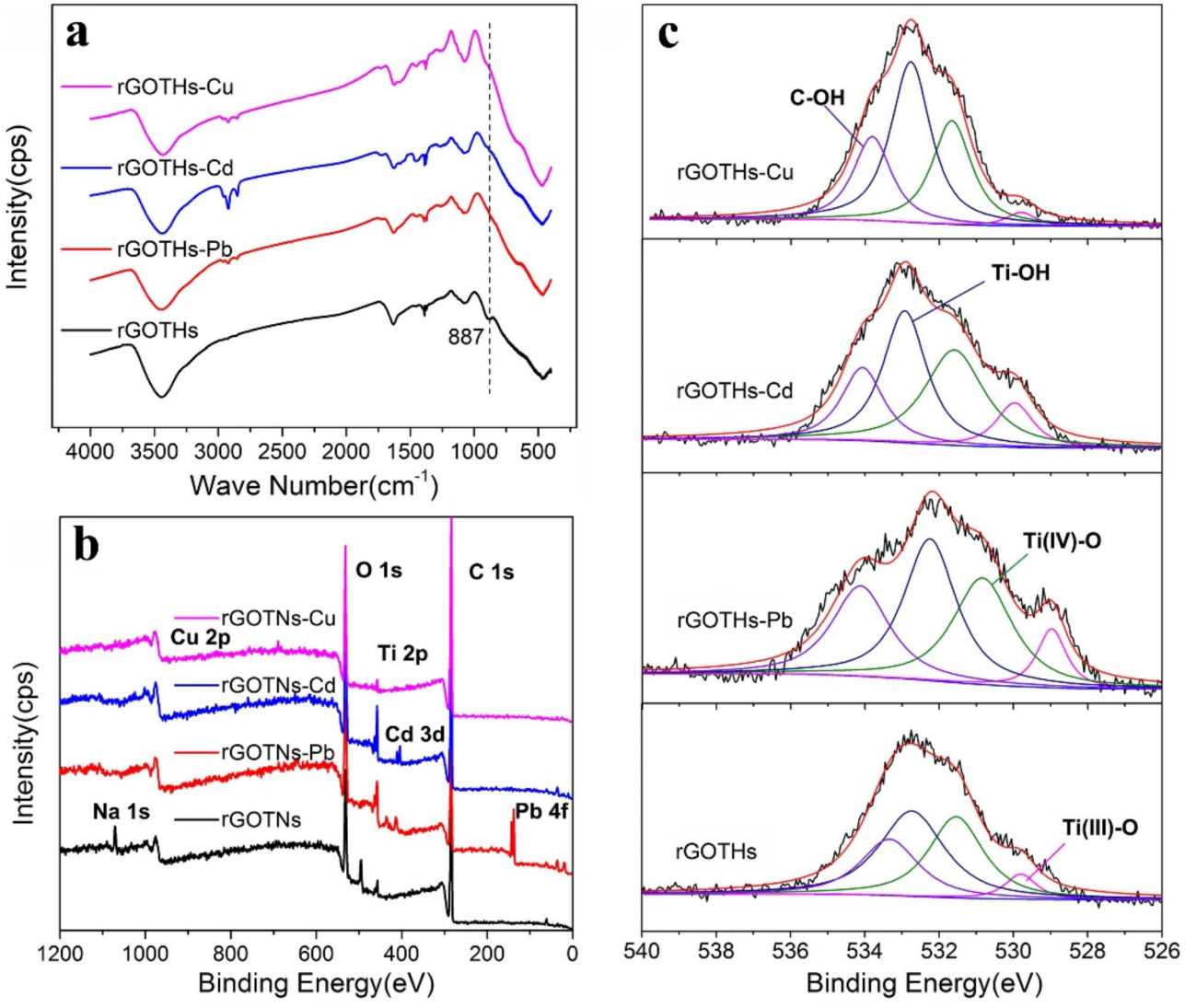

Fig. 7 (**a**) FTIR spectra, (**b**) XPS survey and (**c**) high resolution spectra of O 1s of Pb(II), Cd(II), Cu(II)-sorbed and raw rGOTHs15

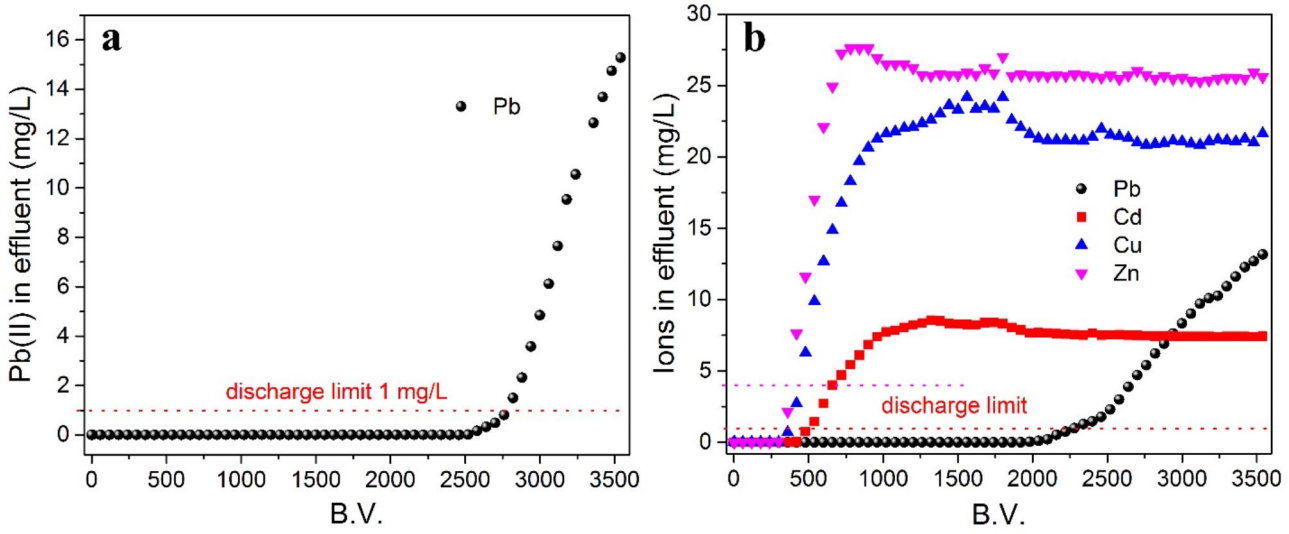

Fig. 8 Breakthrough curves of heavy metals removal by rGOTHs15-packed column process: (**a**) removal of Pb(II) from simulated battery wastewater, (**b**) removal of Pb(II), Cd(II), Cu(II) and Zn(II) from simulated industrial area estuary wastewater

in the adsorption process. As the high-resolution scans for O 1s (Fig. 7c), for rGOTHs15, the peaks at 531.5 eV, 529.8 eV, 532.7 eV and 533.3 eV can be assigned to the lattice oxygen Ti(IV)-O, Ti(III)-O, surface Ti-OH and C-O associated with GO, respectively [32, 52]. The three peaks associated with Ti-O show a significant transformation, suggesting the existence of electrostatic adsorption towards heavy metals with electrons donated by oxygen atoms. Notably, the shift of above peaks are more prominant after Pb(II) adsorption (moved to 529.0 eV, 530.8 eV and 532.3 eV). The results suggest that rGOTHs15 possessed the stronger interaction to Pb(II) than Cd(II) and Cu(II). The binding energy of C-O (533.3 eV) is slightly increased to 534.1 eV, 534.1 eV and 533.8 eV after adsorption of Pb(II), Cd(II) and Cu(II) respectively, indicating that the oxygen-contain groups from rGO components contribute to the removal of heavy metals by coordination.

Treatment of simulated actual battery and estuary wastewater

Dynamic adsorption treatment to two simulated actual wastewater from Wuhan Intepower Co. Ltd, China [53] and Cochin estuary, Kerala state, India [54] were conducted with rGOTHs15-packed fixed bed column (2 g placed in one column). The heavy metals concentrations are given in Sect. 2.4. The column is 12 mm in diameter and 100 mm in length with quartz wool plugging in the end. The effective bed volume was calculated to be 5.6 mL. The empty bed contact time (EBCT) was maintained at 4 min (flow rate of 1.4 mL/min) by a peristaltic pump. The flow rate, empty bed contact time (EBCT), and bed volume for the fixed-bed column experiments were selected based on practical relevance, adsorption kinetics, and scalability considerations. The chosen values align with those reported in previous studies [18].

As shown in Fig. 8a, for single Pb(II) polluted battery manufactory wastewater, the effective treatment volume are 2520 BV (14.11 L) and 2760 BV (15.45 L) for Pb(II) under the discharge limit of 0.1 mg/L and 1 mg/L, while the corresponding breakthrough capacity was 215.5 mg/g and 236.1 mg/g, respectively. For multiple heavy metal polluted estuary effluent (Pb(II), Cd(II), Cu(II), Zn(II)), rGOTHs15-packed column exhibits selective adsorption towards Pb(II) among other coexisting metal ions, with effective treatment reaching 1980 BV (11.08 L) and 2280 BV (12.76 L) for Pb(II) under the discharge limit of 0.1 mg/L and 1 mg/L, while the corresponding breakthrough capacity were 162.6 mg/g and 187.2 mg/g, respectively (Fig. 8b). Under the discharge limit, the effective treatment volume are 420 BV (2.35 L) for Cd(II), 360 BV (2.01 L) for Cu(II), 360 BV (2.01 L) for Zn(II), respectively. rGOTHs15 possesses more superior performance in column dynamic adsorption treatment than traditional activated carbon adsorbent, showing great potential in its practical application.

In the fixed bed system, our rGOTHs-packed column can endure high flow rates, pressure drops and prolonged exposure to harsh chemical environments. As shown in Fig. S9, the exhausted rGOTHs-packed column exhibits no obvious structure damage and the microstructure of rGOTHs also shows no change, implying the excellent mechanical stability of rGOTHs in the fixed bed system. However, when scaling up to commercial applications, the scalability of rGOTHs preparation should be taken into consideration.

Conclusions

In this study, rGO@titanate hybrids were synthesized by alkaline hydrothermal process of graphene oxide supported $Ti(OH)_x$. The prepared rGOTHs could be feasibly separated after adsorption by precipitation and suitable for batch and fixed bed adsorption, owing to the large size as hundreds of microns. More importantly, rGOTHs nanocomposites presented fast adsorption rate and high adsorption capacity towards heavy metals from wastewater. The removal efficiency could be almost reserved even after six cycles. FTIR and XPS studies proved that ion exchange, electrostatic interaction and coordination were the main adsorption mechanism for the adsorption of heavy metals. rGOTHs presented high selective adsorption towards Pb(II) than other ions. In summary, rGOTHs possessed high efficiency, excellent recyclability and feasibility of fixed bed process in removing heavy metals demonstrating great potential for practical application in wastewater treatment. However, lack of real heavy metals-contaminated wastewater samples and parameter optimization such as flow rate, empty bed contact time (EBCT), and bed volume in fixed-bed column, hinder the commercial application of rGOTHs at present. This will be further studied in our future work.

Supplementary Information

The online version contains supplementary material available at https://doi.org/10.1186/s13065-025-01443-z.

Supplementary Material 1

Acknowledgements
The authors thank the Public Technology Center from Northeast Institute of Geography and Agroecology, Chinese Academy of Sciences, for the facilities support.

Author contributions
XTY: experiments design, material synthesis and characterization, adsorption experiments perform, data analysis, original manuscript writing; PL: data analysis, scientific discussion, supervision, manuscript reviewing; HWY: conceptualization, validation, manuscript reviewing, project administration. All authors have approval the final version of the manuscript.

Funding
This work was supported by the Project of Science Development Plan of Jilin Province (Grant, No. YDZJ202201ZYTS488 and No. 20230508158RC), and the Strategic Priority Research Program of the Chinese Academy of Sciences (Grant No. XDA28010502).

Data availability
The datasets used and/or analyzed in this study can be obtained upon request from the corresponding author.

Declarations

Ethics approval and consent to participate
Not applicable.

Consent for publication
Not applicable.

Competing interests
The authors declare no competing interests.

Received: 5 December 2024 / Accepted: 3 March 2025
Published online: 17 March 2025

References

1. Gong Y, Wang Y, Lin N, Wang R, Wang M, Zhang X. Iron-based materials for simultaneous removal of heavy metal(loid)s and emerging organic contaminants from the aquatic environment: recent advances and perspectives. Environ Pollut. 2022;299:118871.
2. Liu M, Almatrafi E, Zhang Y, Xu P, Song B, Zhou C, Zeng G, Zhu Y. A critical review of biochar-based materials for the remediation of heavy metal contaminated environment: applications and practical evaluations. Sci Total Environ. 2022;806:150531.
3. Kumar A, Virender M, Saini B, Mohan, Shayoraj, Kamboj M. Colorimetric and fluorescent schiff base sensors for trace detection of pollutants and biologically significant cations: A review (2010–2021). Microchem J. 2022;181:107798.
4. Liu M, Liu Y, Shen J, Zhang S, Liu X, Chen X, Ma Y, Ren S, Fang G, Li S, Li CT, Sun T. Simultaneous removal of Pb^{2+}, Cu^{2+} and Cd^{2+} ions from wastewater using hierarchical porous polyacrylic acid grafted with lignin. J Hazard Mater. 2020;392:122208.
5. Ji C, Wu D, Lu J, Shan C, Ren Y, Li T, Lv L, Pan B, Zhang W. Temperature regulated adsorption and desorption of heavy metals to A-MIL-121: mechanisms and the role of exchangeable protons. Water Res. 2021;189:116599.
6. Du J, Shang X, Shi J, Guan Y. Removal of chromium from industrial wastewater by magnetic flocculation treatment: experimental studies and PSO-BP modelling. J Water Process Eng. 2022;47:102822.
7. Sun M, Qin M, Wang C, Weng G, Huo M, Taylor AD, Qu J, Elimelech M. Electrochemical-Osmotic process for simultaneous recovery of electric energy, water, and metals from wastewater. Environ Sci Technol. 2020;54:8430–42.
8. Ayalew ZM, Zhang X, Guo X, Ullah S, Leng S, Luo X, Ma N. Removal of Cu, Ni and Zn directly from acidic electroplating wastewater by Oligo-Ethyleneamine dithiocarbamate (OEDTC). Sep Purif Technol. 2020;248:117114.
9. Yimer M, Ansari SN, Berehe BA, Gudimella KK, Gedda G, Girma WM, Hasan N, Tasneem S. Adsorptive removal of heavy metals from wastewater using Cobalt-diphenylamine (Co-DPA) complex, BMC chem. 2024;18:23.
10. Gokhale D, Hamelberg AF, Doyle PS. Multifunctional zwitterionic hydrogels for the rapid elimination of organic and inorganic micropollutants from water. Nat Water. 2024;2:62–71.
11. Fei Y, Hu YH. Design, synthesis, and performance of adsorbents for heavy metal removal from wastewater: a review. J Mater Chem A. 2022;10:1047–85.
12. Jawed A, Saxena V, Pandey LM. Engineered nanomaterials and their surface functionalization for the removal of heavy metals: A review. J Water Process Eng. 2020;33:101009.
13. Singh AR, Mohan B, Raghav N, Sagar, Virender, Abhishek, and, Pombeiro AJL. Understanding the mechanisms and applications of luminescent covalent organic frameworks (COFs) for multi-analyte sensing, J. Mol. Struct. 2025;1321:139945.
14. Mohan B, Virender RK, Gupta AJL, Pombeiro, Ren P. Advanced luminescent metal-organic framework (MOF) sensors engineered for urine analysis applications. Coordin Chem Rev. 2024;519:216090.
15. Zhao W, Chen IW, Xu F, Huang F. A novel ultralight three-dimensional house-of-cards Titania monolith for extraordinary heavy-metal adsorption. J Mater Chem A. 2017;5:15724–9.
16. Polonini HC, Brandao HM, Raposo NRB, Mouton L, Yepremian C, Coute A, Brayner R. Ecotoxicological studies of micro- and nanosized barium titanate on aquatic photosynthetic microorganisms. Aquat Toxicol. 2014;154:58–70.
17. Sounthararajah DP, Loganathan P, Kandasamy J, Vigneswaran S. Adsorptive removal of heavy metals from water using sodium titanate nanofibres loaded onto GAC in fixed-bed columns. J Hazard Mater. 2015;287:306–16.
18. Wei Y, Wei S, Liu C, Chen T, Tang Y, Ma J, Yin K, Luo S. Efficient removal of arsenic from groundwater using iron oxide nanoneedle array-decorated Biochar fibers with high Fe utilization and fast adsorption kinetics. Water Res. 2019;167:115107.
19. Atmianlu PA, Badpa R, Aghabalaei V, Baghdadi M. A review on the various beds used for immobilization of nanoparticles: overcoming the barrier to nanoparticle applications in water and wastewater treatment. J Environ Chem Eng. 2021;9:106514.

20. Ahmad SZN, Salleh WNW, Ismail AF, Yusof N, Yusop MZM, Aziz F. Adsorptive removal of heavy metal ions using graphene-based nanomaterials: toxicity, roles of functional groups and mechanisms. Chemosphere. 2020; 248:126008.
21. Liu X, Ma R, Wang X, Ma Y, Yang Y, Zhuang L, Zhang S, Jehan R, Chen J, Wang X. Graphene oxide-based materials for efficient removal of heavy metal ions from aqueous solution: A review. Environ Pollut. 2019;252:62–73.
22. Bao S, Yang W, Wang Y, Yu Y, Sun Y. One-pot synthesis of magnetic graphene oxide composites as an efficient and recoverable adsorbent for Cd(II) and Pb(II) removal from aqueous solution. J Hazard Mater. 2020;381:120914.
23. Vazquez-Jaime M, Arcibar-Orozco JA, Damian-Ascencio CE, Saldana-Robles AL, Martinez-Rosales M, Saldana-Robles A, Cano-Andrade S. Effective removal of arsenic from an aqueous solution by ferrihydrite/goethite graphene oxide composites using the modified hummers method. J Environ Chem Eng. 2020;8:104416.
24. Wan S, Ding W, Wang Y, Wu J, Gu Y, He F. Manganese oxide nanoparticles impregnated graphene oxide aggregates for cadmium and copper remediation. Chem Eng J. 2018;350:1135–43.
25. Zhao G, Li J, Ren X, Chen C, Wang X. Few-Layered graphene oxide nanosheets as superior sorbents for heavy metal ion pollution management. Environ Sci Technol. 2011;45:10454–62.
26. Hao L, Song H, Zhang L, Wan X, Tang Y, Lv Y. SiO_2/graphene composite for highly selective adsorption of Pb(II) ion. J Colloid Interf Sci. 2012;369:381–7.
27. Huang Q, Chen Y, Yu H, Yan L, Zhang J, Wang B, Du B, Xing L. Magnetic graphene oxide/MgAl-layered double hydroxide nanocomposite: One-pot solvothermal synthesis, adsorption performance and mechanisms for Pb^{2+}, Cd^{2+}, and Cu^{2+}. Chem Eng J. 2018;341:1–9.
28. Lellala K, Behera SK, Srivastava P, Saeed WS, Haidyrah AS, Burile AN. Fe_3O_4 nanoparticles decorated on N-doped graphene oxide nanosheets for elimination of heavy metals from industrial wastewater and desulfurization. Diam Relat Mater. 2024;150:111746.
29. Bi J, Huang X, Wang J, Tao Q, Wang T, Hao H. Titanate for water remediation: synthesis, application, mechanism and optimization. J Mater Chem A. 2020;8:14415–40.
30. Li H, Huang Y, Liu J, Duan H. Hydrothermally synthesized titanate nanomaterials for the removal of heavy metals and radionuclides from water: A review. Chemosphere. 2021;282:131046.
31. Wang L, Badr HO, Yang Y, Cope JH, Ma E, Ouyang J, Yuan L, Li Z, Liu Z, Barsoum MW, Shi W. Unique hierarchical structures of one dimensional lepidocrocite titanate with cation-exchangeable sites for extraordinary selective actinide capture for water purification. Chem Eng J. 2023;474:145635.
32. Thuy-Duong N-P, Viet Hung P, Kim EJ, Oh E-S, Hur SH, Chung JS, Lee B, Shin EW. Reduced graphene oxide-titanate hybrids: morphologic evolution by alkali-solvothermal treatment and applications in water purification. Appl Surf Sci. 2012;258:4551–7.
33. Sun S, Huang X, Bi J, Wang N, Wang T, Zhou L, Wang L, Lamichhane S, Hao H. Enhanced ion recognition through bi-directionally layered spacing regulation of 1D tubular titanate nanofilms. Chem Eng J. 2023;468:143594.
34. Li K, Hanpei Y, Lina W, Siqi C, Ruichen Z, Junming W, Xiaona L. Facile integration of FeS and titanate nanotubes for efficient removal of total cr from aqueous solution: synergy in simultaneous reduction of cr(VI) and adsorption of cr(III). J Hazard Mater. 2020;398:122834.
35. Pitiphattharabun S, Auewattanapun K, Htet TL, Thu MM, Panomsuwan G, Techapiesancharoenkij R, Ohta J, Jongprateep O. Reduced graphene oxide/zinc oxide composite as an electrochemical sensor for acetylcholine detection. Sci Rep. 2024;14:14224.
36. Xie T, Wang Y, Zhang Q, Guo W, Shen S, Wang Q, Chen X, Qu L, Li C. $Ti_3C_2T_x$ MXene-derived hydroxyl-rich titanate based hybrid membrane with cellulose as structural regulator for highly-efficient disposition of heavy metal ions. Desalination. 2024;572:117115.
37. Gu P, Zhang S, Zhang C, Wang X, Khan A, Wen T, Hu B, Alsaedi A, Hayat T, Wang X. Two-dimensional MAX-derived titanate nanostructures for efficient removal of Pb(II). Dalton T. 2019;48:2100–7.
38. Ma J, Li F, Qian T, Liu H, Liu W, Zhao D. Natural organic matter resistant powder activated charcoal supported titanate nanotubes for adsorption of Pb(II). Chem Eng J. 2017;315:191–200.
39. Wei J, Ge L, Wang W, Hong P, Li Y, Li Y, Xie C, Wu Z, He J, Kong L. Efficient remediation of heavy metal-contaminated water using a magnetically collectible nanoscale Cu/Fe/rGO primary battery. J Environ Chem Eng. 2024;12:111574.
40. Lai KC, Lee LY, Hiew BYZ, Thangalazhy-Gopakumar S, Gan S. Facile synthesis of Xanthan biopolymer integrated 3D hierarchical graphene oxide/titanium dioxide composite for adsorptive lead removal in wastewater. Bioresour Technol. 2020;309:123296.
41. Yap PL, Auyoong YL, Hassan K, Farivar F, Tran DNH, Ma J, Losic D. Multithiol functionalized graphene bio-sponge via photoinitiated thiol-ene click chemistry for efficient heavy metal ions adsorption. Chem Eng J. 2020;395:124965.
42. Jiang H, Yang Y, Lin Z, Zhao B, Wang J, Xie J, Zhang A. Preparation of a novel bio-adsorbent of sodium alginate grafted polyacrylamide/graphene oxide hydrogel for the adsorption of heavy metal ion. Sci Total Environ. 2020;744:140653.
43. Fu W, Huang ZQ. Magnetic dithiocarbamate functionalized reduced graphene oxide for the removal of Cu(II), Cd(II), Pb(II), and Hg(II) ions from aqueous solution: synthesis, adsorption, and regeneration.Chemosphere. 2018;209:449–56.
44. Kong L, Li Z, Huang X, Huang S, Sun H, Liu M, Li L. Efficient removal of Pb(ii) from water using magnetic Fe_3S_4/reduced graphene oxide composites. J Mater Chem A. 2017;5:19333–42.
45. Pourbeyram S. Effective removal of heavy metals from aqueous solutions by graphene Oxide-Zirconium phosphate (GO-Zr-P) nanocomposite. Ind Eng Chem Res. 2016;55:5608–17.
46. Wang T, Liu W, Xiong L, Xu N, Ni J. Influence of pH, ionic strength and humic acid on competitive adsorption of Pb(II), Cd(II) and Cr(III) onto titanate nanotubes. Chem Eng J. 2013;215:366–74.
47. Liu W, Wang T, Borthwick AGL, Wang Y, Yin X, Li X, Ni J. Adsorption of Pb^{2+}, Cd^{2+}, Cu^{2+} and Cr^{3+} onto titanate nanotubes: competition and effect of inorganic ions. Sci Total Environ. 2013;456–7:171–180.
48. Maslova M, Ivanenko V, Yanicheva N, Gerasimova L. The effect of heavy metal ions hydration on their sorption by a mesoporous titanium phosphate ion-exchanger. J Water Process Eng. 2020;35:101233.
49. Yang X, Zhu G, Liu Y, Wang Q, Guo N, Zeng Y, Han X, Yu D, Yu H. Enhanced removal of Pb(II) from contaminated water by hierarchical titanate microtube derived from titanium glycolate. Adv Powder Technol. 2022;33:103376.
50. Ali DA, Ali RG. Green synthesis of carbonized Chitosan-Fe_3O_4-SiO_2 nanocomposite for adsorption of heavy metals from aqueous solutions. BMC Chem. 2024;18:147.
51. Bi J, Huang X, Wang J, Tao Q, Lu H, Luo L, Li G, Hao H. Self-assembly of immobilized titanate films with different layers for heavy metal ions removal from wastewater: synthesis, modeling and mechanism. Chem Eng J. 2020;380:122564.
52. Lei X, Li X, Ruan Z, Zhang T, Pan F, Li Q, Xia D, Fu J. Adsorption-photocatalytic degradation of dye pollutant in water by graphite oxide grafted titanate nanotubes. J Mol Liq. 2018;266:122–31.
53. Wang N, Xu X, Yang L, Yuan L, Xiao T, Li H, Yu H. Plate column adsorption of Pb(II) from industrial wastewater on sponge-type composite adsorbent: optimization and application. J Ind Eng Chem. 2018;66:333–42.
54. Dev VV, Baburaj G, Antony S, Arun V, Krishnan KA. Zwitterion-chitosan bed for the simultaneous immobilization of Zn(II), Cd(II), Pb(II) and Cu(II) from multimetal aqueous systems. J Clean Prod. 2020;255:120309.

Publisher's note